Methods

Generation of mice expressing thrombin cleavage-resistant osteopontin (*Spp1*$^{R153A/R153A}$)

To create a R153A knock-in point mutation in the gene encoding osteopontin (OPN; secreted phosphoprotein 1, *Spp1*) that prevents thrombin cleavage of OPN in mice, we used homologous recombination in mouse embryonic stem (ES) cells derived from C57BL/6J mice and subsequent blastocyst injection of the appropriate targeted ES cells (Supplementary Figure 1). The methods used ensured that expression of OPN was still under the control of the wild type regulatory elements which was confirmed by Southern blot and sequencing analysis on the resulting mice (see below).

The *Spp1* gene sequence (nucleotides 104,834,137~104,900,066) was retrieved from the Ensembl database and used as reference. Mouse RP23-410M1 BAC DNA was used for generating the homology arms for the gene targeting vector, and Southern probes for screening the targeted events. The 5' homology arm (~5.0 kb) and the 3' homology arm (~2.5 kb) were both generated by PCR. The R153A point mutation, located in exon 5 of the 3' homology arm, was introduced by site-directed mutagenesis. These fragments were cloned into the LoxNwCD vector and confirmed by restriction digestion and end-sequencing.

The final vector also contained loxP sequences flanking the Neo expression cassette (for positive selection of the ES cells), and a diphtheria toxin A (DTA) expression cassette (for negative selection of the potentially targeted ES cells). It was confirmed by restriction endonuclease digestion and end sequencing analysis. The final vector was linearized with NotI prior to electroporation.

5' and 3' external probes were generated by PCR, cloned in the pCR4.0 backbone, confirmed by sequencing and tested by genomic Southern analysis for screening the ES cells.

NotI-linearized final vector DNA (30 μg) was electroporated into ~10^7 C57BL/6J ES cells and selected with 200 μg/ml G418. 192 ES cell clones were screened by PCR and five potential targeted clones were selected for further

analysis. Upon completion of the ES clone expansion, Southern and PCR/sequencing confirmation analysis was performed and showed that two clones (E9 and F8) were correctly targeted with a single neo insertion.

Male chimeras were generated after blastocyst injection of clones E9 and F8: 99% (n=1), 90% (n=1), 80% (n=2), 70% (n=2), 60% (n=1), 50% (n=1), 40% (n=1), 30% (n=1), and 20% (n=1) which were bred with C57BL/6J WT females to generate heterozygotes identified by PCR analysis. Back-crosses with C57BL/6J mice generated homozygous mice carrying the mutant *Spp1* gene identified by PCR analysis (Supplementary Figure 2) using primers in Supplementary Table 1. ES cell work was performed by Caliper Discovery Alliances and Services (Hanover, MD).

Cell culture

B16-F10 (mouse melanoma, CRL6475), Yumm3.1 (1) (mouse melanoma with BrafV600E/wt Cdkn2$^{-/-}$, CRL3365) and RAW 264.7 (mouse macrophage, TIB) cell lines were obtained from ATCC (Manassas, VA) and cultured in DMEM (Corning, NY) in the presence of 5% fetal bovine serum (FBS) with penicillin-streptomycin-glutamine (Gibco Life Technologies, Langley, OK). Testing by Idexx (Sacramento, CA) showed the cells were uncontaminated. Cells were used within 5 passages of receipt.

Collection of tumors

Animals were euthanized using CO_2 and blood collected by cardiac puncture. Tumors were carefully isolated, weighed and in some experiments tumor volume was also determined after sacrifice with calipers. Part of the tumor was stored in formaldehyde for immunohistochemistry, part was frozen and stored at -80°C for preparation of tumor lysates for OPN ELISAs. Tumor lysates were prepared by homogenizing the tumor samples in RIPA buffer (Pierce, Carlsbad, CA) with complete protease inhibitor cocktail (Roche, Indianapolis-Marion County, Indiana). Protein concentration was determined by Bio-Rad Protein Assay (Bio-Rad, Hercules, CA).

Histology and immunohistochemistry

Standard histology and immunostaining protocols were performed, and investigators were blinded during histologic staining. 4% paraformaldehyde was used as the fixative. Briefly, immunofluorescence analysis was performed on 5-10 μm-thick sections of mouse melanoma tumor. The following primary antibodies were used: rat anti-mouse F4/80 monoclonal antibody (Bio-Rad, #MCA497RT) and rabbit anti-mouse CD3 polyclonal antibody (Abcam, #5690). Immune complexes were detected with secondary antibodies conjugated with Alexa Fluor 488 (Abcam, #Ab150157). A DAPI counterstain was used. After staining, images were directly analyzed using a Keyence imaging system. A minimum of 4-6 sections was stained per sample. Secondary antibody only control was included for every experiment. Representative images were selected for figure panels.

Melanin determination

The left lobe of lung from each mouse from the metastasis model was weighed and incubated in 1M NaOH/10% DMSO for 2 hr at 80°C before centrifugation (12,000 rpm) for 10 min at room temperature. Melanin content was determined by measuring the absorbance of the supernatant at 470 nm and comparing it to a standard curve of synthetic melanin (Sigma, St. Louis, MO), and expressed as μg/mg protein determined by protein assay of lung tissue.

Preparation of plasma and bone marrow cells

Plasma samples were prepared from mice by collection of blood *via* cardiac puncture into 3.2% sodium citrate with 9:1 blood to citrate ratio (v/v). Blood was centrifuged at 2500 rpm for 20 min. to prepare plasma and stored at -80°C. Bone marrow cells were prepared as described previously (2).

Clinical chemistry

Clinical chemistry analysis was carried out on plasma from male and female WT, OPN-KI and OPN-KO mice at Idexx Laboratories Inc (Sacramento CA).

Complete blood counts

Complete blood counts (CBC) were carried out on male and female WT, OPN-KI and OPN-KO mice at different ages from 5 weeks to 26 weeks at Idexx Laboratories Inc.

Cell adhesion assay

Wells in 96-well plate was coated with either BSA or different OPN fragments (20 nM) in coating buffer (Gibco Life Technologies, Langley, OK) and incubated at 4°C overnight. The plate was washed thrice with PBS and blocked with 3% BSA for 1 hr. B16 or RAW cells ($2x10^6$) in 1X HBSS containing 0.2 mM $MnCl_2$ were added to the wells and incubated at 37°C for 1 hr. Wells were washed and cells fixed with absolute ethanol for 20 min and stained with 0.1% crystal violet. Cells were washed repeatedly with PBS until no violet color was visible, lysed with 0.5% Triton X-100 and absorbance determined at 570 nm. The value for BSA, used as the negative control, was compared to all other samples by one-way ANOVA followed by Dunnett's test.

Cell growth assay

B16 cells ($5x10^4$) were plated in 12-well plate in DMEM without serum containing OPN fragments or BSA (10 nM). After 24 hr at 37 °C, cells were trypsinized and counted. The growth ratio was calculated by normalizing to the cell count for BSA. The value for BSA, used as the negative control, was compared to all other samples by one-way ANOVA followed by Dunnett's test.

Apoptosis assay

B16 cells ($1x10^5$) were cultured in DMEM without serum overnight. Camptothecin (Abcam, Burlingame, CA) (20 μM) was added in the presence of BSA (negative control) or OPN fragments (10 nM). After 4 hr incubation, binding buffer was added, the plate centrifuged at 400 g for 5 min and supernatant discarded. Annexin V FITC stain (Cayman chemicals, Ann Arbor, MI) was added to the cells and incubated for 10 min in the dark. Cells were centrifuged, binding buffer added and fluorescence intensity measured at 485/535 nm (excitation/emission). The apoptotic index was calculated by dividing the value for the camptothecin-treated cells with that from untreated

cells. The value for BSA, used as the negative control, was compared to all other samples by one-way ANOVA followed by Dunnett's test.

Cell migration assay

B16 cells (10^5) were placed in the upper chamber of a 6.5 mm transwell with a pore size of 8.0 μm (Sigma). The lower chamber was filled with BSA or various OPN fragments (10 nM) in presence of 0.2 mM $MnCl_2$ (Sigma) and incubated at 37°C for 24 hr. Cells that migrated to the lower chamber were centrifuged and resuspended in 1X HBSS (Gibco Life Technologies, Langley, OK) with CCK-8 staining solution (Dojindo Molecular Technologies Inc., Rockville, MD), incubated for 2 hr and absorbance at 450 nm measured. The value for BSA, used as the negative control, was compared to all other samples by one-way ANOVA followed by Dunnett's test.

PGE_2 assay

RAW cells ($5x10^5$) were plated onto 6-well plate in serum-free medium with either BSA or various OPN fragments (10 nM). After overnight culture, PGE_2 levels in cell-cultured media were determined by ELISA (Enzo, Farmingdale, NY). BSA, used as the negative control, with values subtracted from the values for the OPN fragments.

Analysis of integrin expression

B16 or RAW cells were labeled with anti-mouse integrin α_4 antibody, anti-mouse integrin α_9 antibody, anti-mouse integrin β_1 antibody or isotype control antibodies, for analysis by flow cytometry.

Flow cytometric analysis of leukocytes

Tumors were isolated, weighed and dissociated with Tumor Dissociation Kit (Miltenyi Biotec, Auburn, CA) and gentleMACS Octo Dissociator with Heaters (Miltenyi Biotec) according to the manufacturer's instructions. After dissociation, the cell suspension was filtered with a 40mm filter and subjected to erythrocyte cell lysis using ACK lysis buffer (Lonza, Walkersville, MD). Lysis buffer was inactivated by adding 10 times vol/vol of DMEM

medium containing serum. Cells were centrifuged (300 rcf, 10 min) and gently resuspended in FACS buffer (PBS + 1% BSA) and counted. After blocking Fc with CD16/32 Fc-blocking antibody for 20 min, 10^6 cells were stained for 30 min. at 4°C in the dark with either a mixture of antibodies against CD3**,** CD11b, CD11c, CD19**,** CD38, CD45, CD161, CD206, EGR-2, F4/80, Gr-1, MHC II and Sytox green (3,4), or a mixture of antibodies against CD3, CD19, CD45, and Sytox green. Cells were then washed again with FACS buffer. Compensation Beads (Invitrogen, Waltham, MA) and samples stained with single antibody were used for controls. Cells were analyzed on a flow cytometer (BD LSR II) and data analysis was carried out with FlowJo (Becton Dickinson, San Jose, CA). The gating strategy is shown in Supplementary Figure 3 and antibody source in Supplementary Table 2.

References

1. Meeth K, Wang JX, Micevic G, Damsky W, Bosenberg MW. The YUMM lines: a series of congenic mouse melanoma cell lines with defined genetic alterations. Pigment cell & melanoma research **2016**;29(5):590-7
2. Toda M, Shao Z, Yamaguchi KD, Takagi T, D'Alessandro-Gabazza CN, Taguchi O*, et al.* Differential gene expression in thrombomodulin (TM; CD141)(+) and TM(-) dendritic cell subsets. PLoS One **2013**;8(8):e72392
3. Jablonski KA, Amici SA, Webb LM, Ruiz-Rosado Jde D, Popovich PG, Partida-Sanchez S*, et al.* Novel Markers to Delineate Murine M1 and M2 Macrophages. PLoS One **2015**;10(12):e0145342
4. Weichand B, Popp R, Dziumbla S, Mora J, Strack E, Elwakeel E*, et al.* S1PR1 on tumor-associated macrophages promotes lymphangiogenesis and metastasis via NLRP3/IL-1beta. J Exp Med **2017**;214(9):2695-713

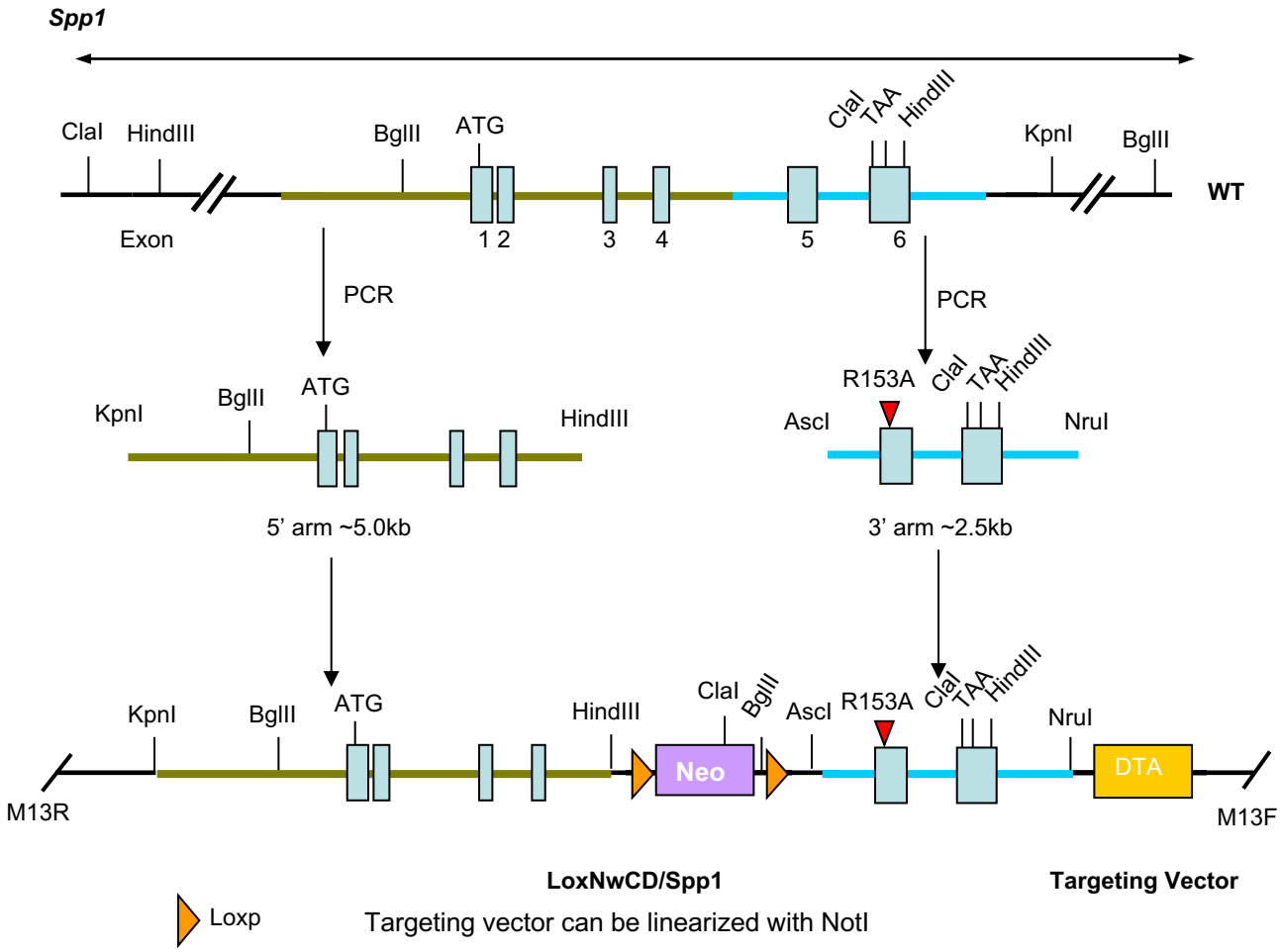

Supplementary Figure 1: Construction of the targeting vector

The construction of the targeting vector is shown. The *Spp1* gene sequence (nucleotides 104,834,137~104,900,066) from mouse chromosome 5 is shown in the WT line (top line). Two plasmids, one with the 5' homology arm (exons 1 - 4) and the 3' homology arm (exons 5 and 6) were constructed. Exon5 containing the codon for amino acid 153 which was mutated from Arg to Ala (R153A; red arrow). These two sequences were then inserted into the targeting vector LoxNwCD along with the Neo cassette flanked by LoxP sites (bottom line, targeting vector). ATG: initiation codon; DTA: diphtheria toxin.

A.

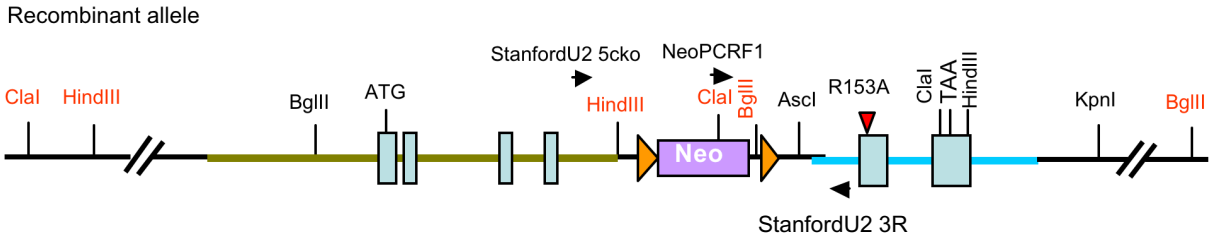

This scheme shows the PCR primer and sequencing primer positions within the recombinant allele

B.

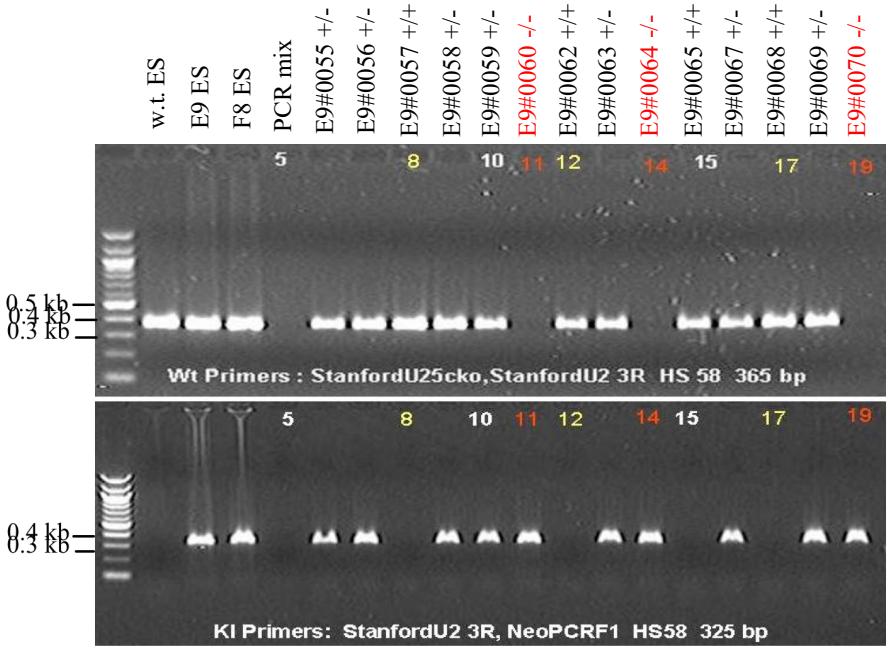

Supplementary Figure 2: Generation of OPN-KI mice

A. Map of recombinant allele showing locations of primers (A). Mice homozygous for the mutated R153A gene (red lettering) were identified by PCR screening (B). The sequence of the primers is shown in Supplementary Table 1.

A.

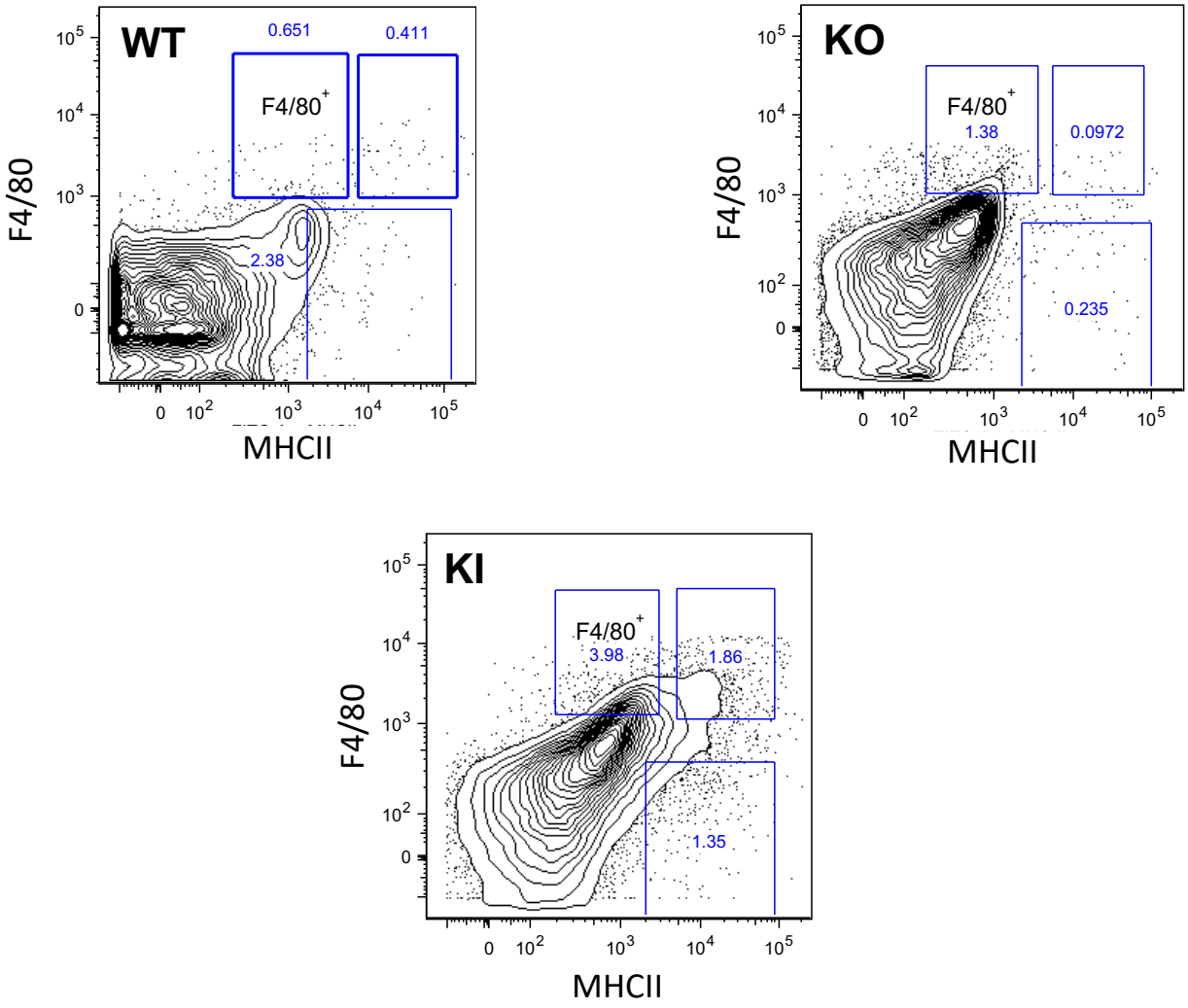
WT
0.651
0.411
F4/80+
2.38
F4/80
MHCII
KO
F4/80+
1.38
0.0972
0.235
F4/80
MHCII
KI
F4/80+
3.98
1.86
1.35
F4/80
MHCII

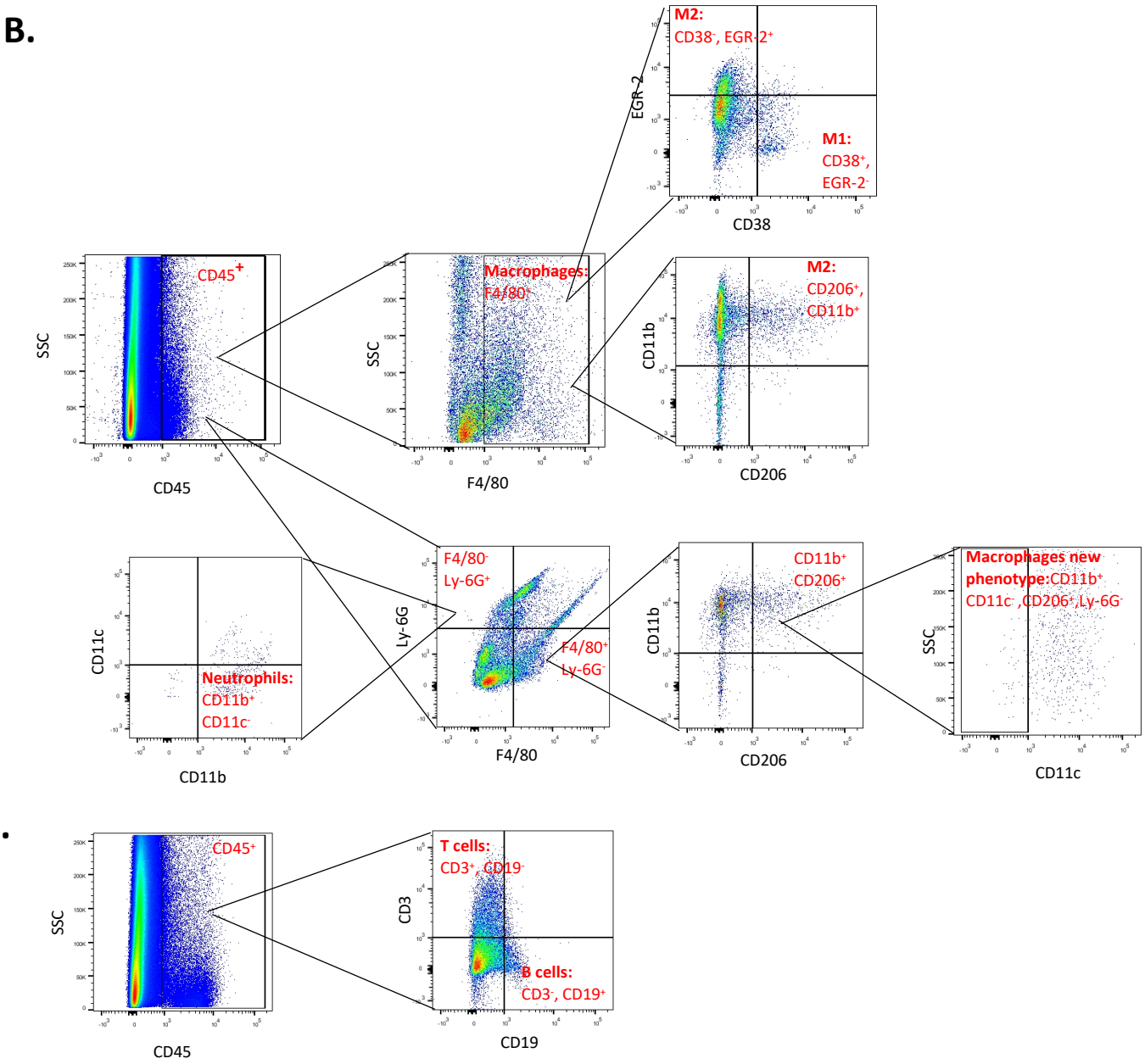

Supplementary Figure 3: Gating strategy for flow cytometry

Gating strategy employed for analysis of F4/80$^+$ cells (A), for tumor-infiltrating macrophages and neutrophils (B) and B and T cells (C).

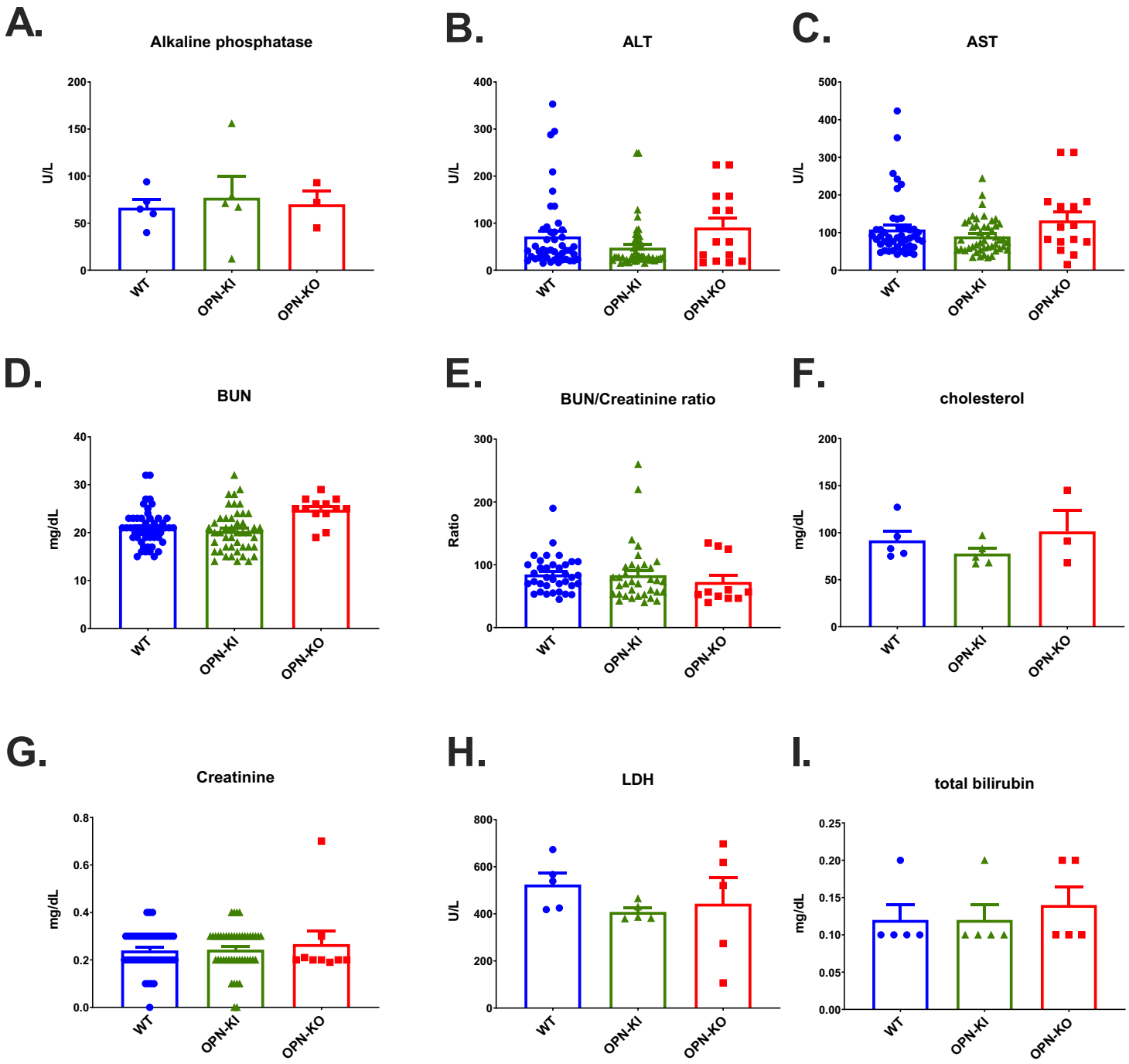

Supplementary Figure 4: No differences between WT, OPN-KI and OPN-KO mice in clinical chemistry

Levels of alkaline phosphatase (A), ALT (B), AST (C), BUN (D), BUN/creatinine ration (E), cholesterol (F), creatinine (G), lactate dehydrogenase (LDH; H) and total bilirubin (I) in plasma from WT, OPN-KI and OPN-KO mice. N>5 for all groups except OPN-KO in panels A and F. All data are shown as mean ± SEM. Data analyzed by ANOVA followed by Tukey's post hoc test and showed no differences between groups.

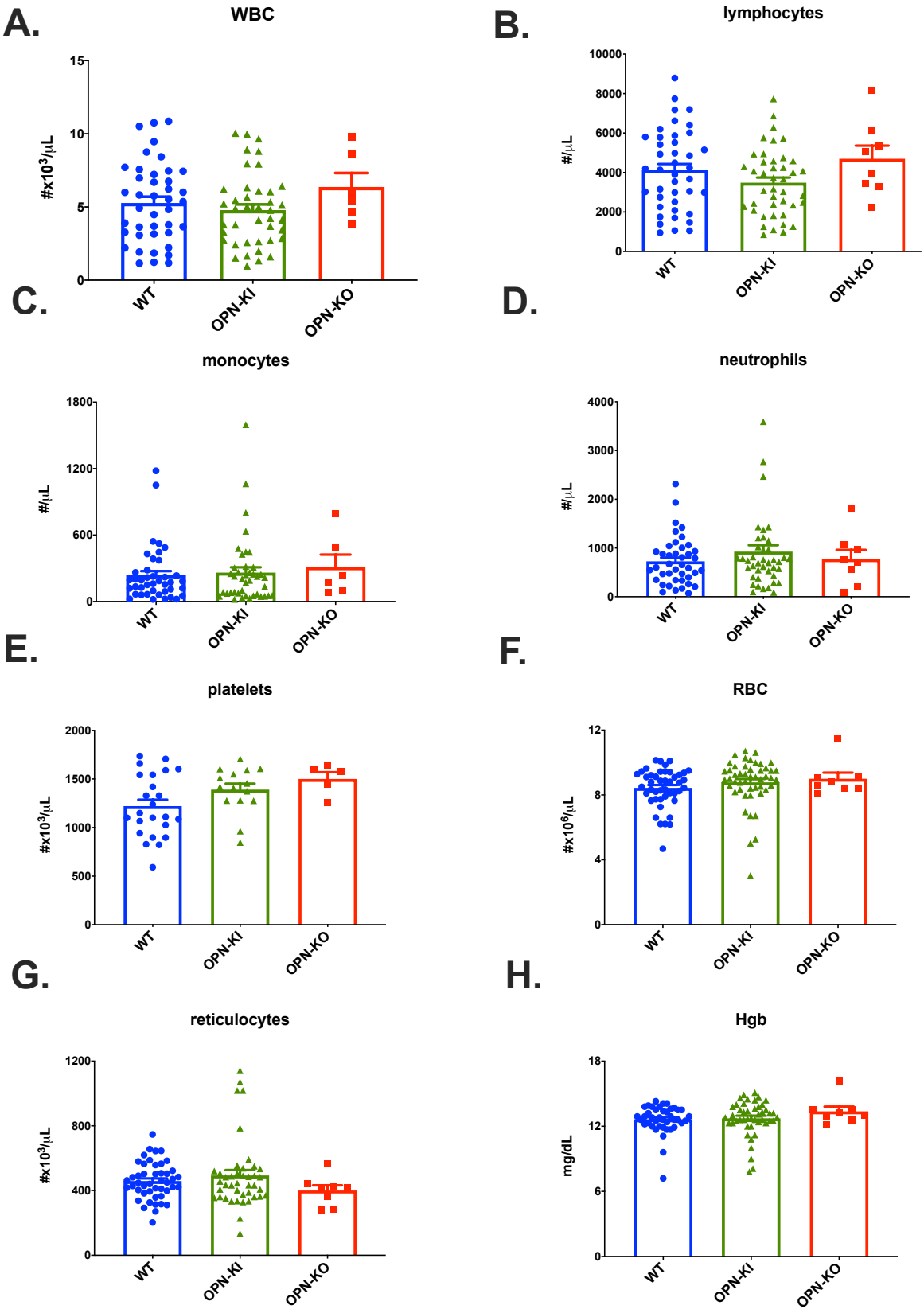

Supplementary Figure 5: No differences between WT, OPN-KI and OPN-KO mice in CBC

Blood cell counts from WT, OPN-KI and OPN-KO mice. Numbers of WBCs (A), lymphocytes (B), monocytes (C), neutrophils (D), platelets (E), RBCs (F), reticulocytes (G) and level of hemoglobin (Hgb: H). All data are

shown as mean ± SEM. N>8. Data analyzed by ANOVA followed by Tukey's post hoc test and showed no differences between groups.

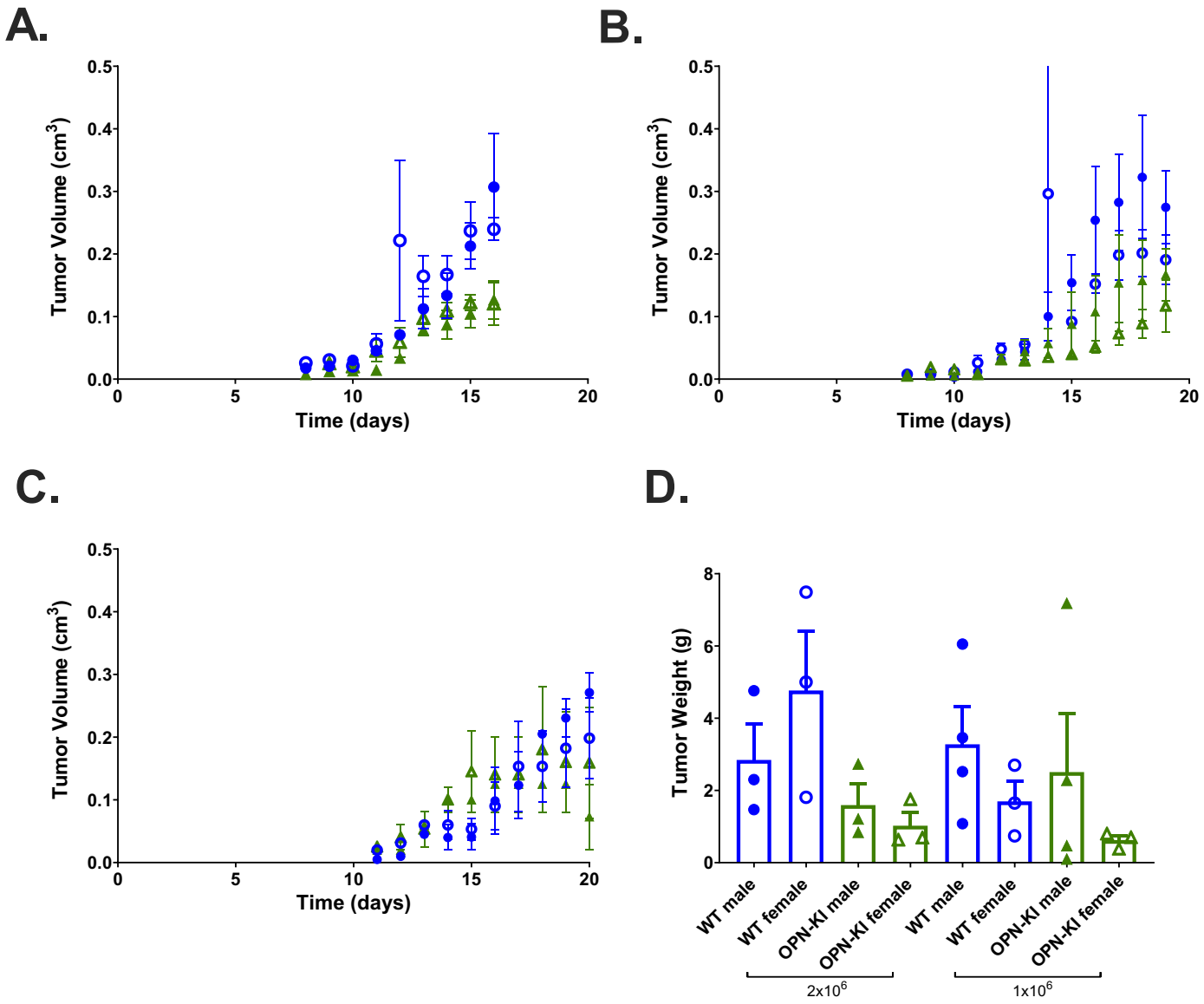

Supplementary Figure 6: No differences in B16 tumor growth between male and female WT and OPN-KI mice nor due to size of inoculum.

Comparison of B16 growth in male (solid symbols) and female (open symbols) WT (blue circles) and OPN-KI (green triangles) mice inoculated with different numbers of cells. (A) $2x10^6$ cells, (B) $1x10^6$ cells, (C) $0.5x10^6$ cells, (D) Weight of B16 tumors after sacrifice in male (solid symbols) and female (open symbols) WT (blue circles) and OPN-KI (green triangles) mice. All data are shown as mean ± SEM. N=3 for each group except for WT male and OPN-KI male ($1x10^6$ cells/mouse) where N=4. Data analyzed by ANOVA followed by Tukey post hoc test and showed no differences between groups.

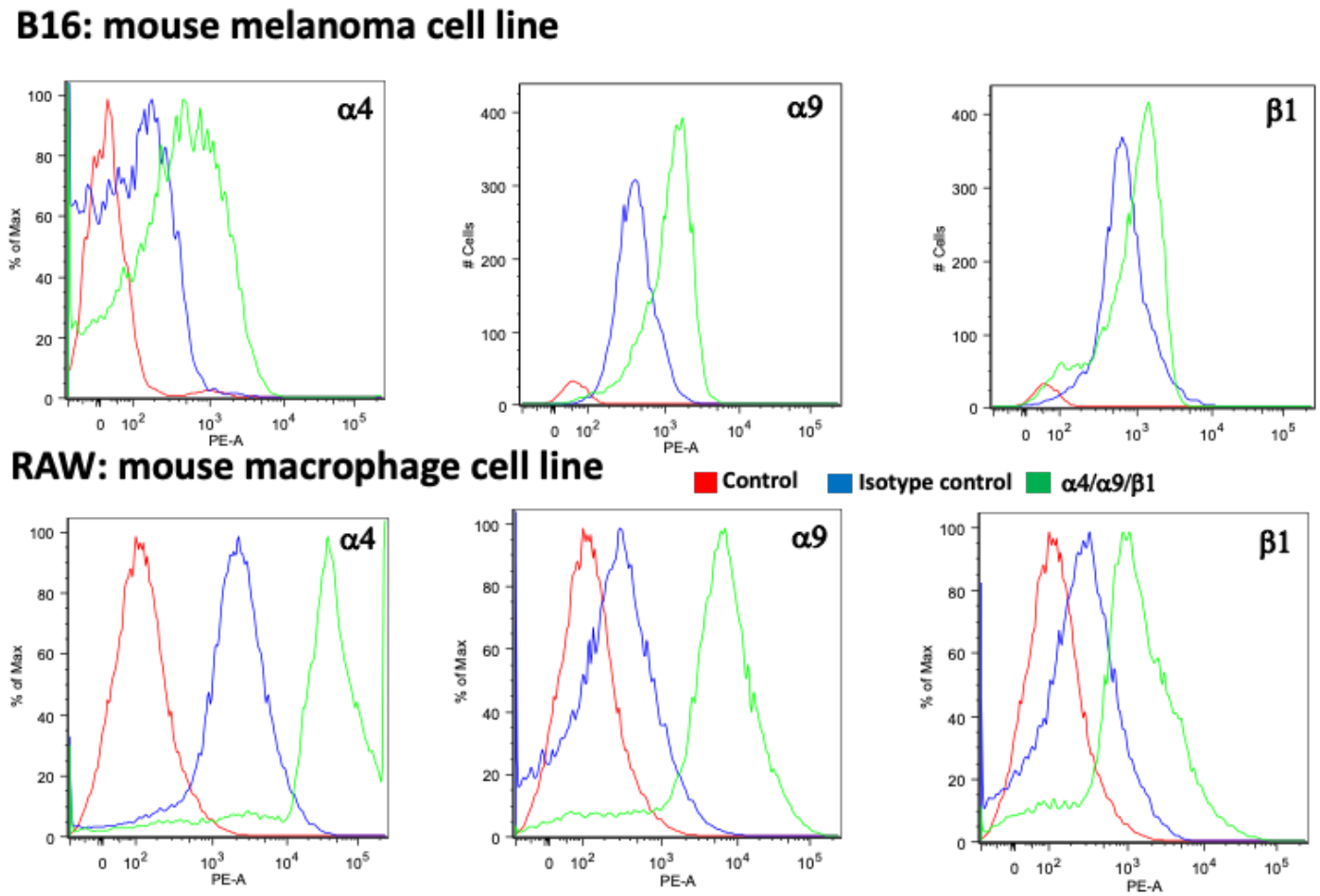

Supplementary Figure 7: α9β1 and α4β1 integrins are expressed on B16 and RAW cells

Expression of α9β1 and α4β1 integrins on B16 and RAW cells by flow cytometry using specific antibodies compared to isotype and unlabeled controls.

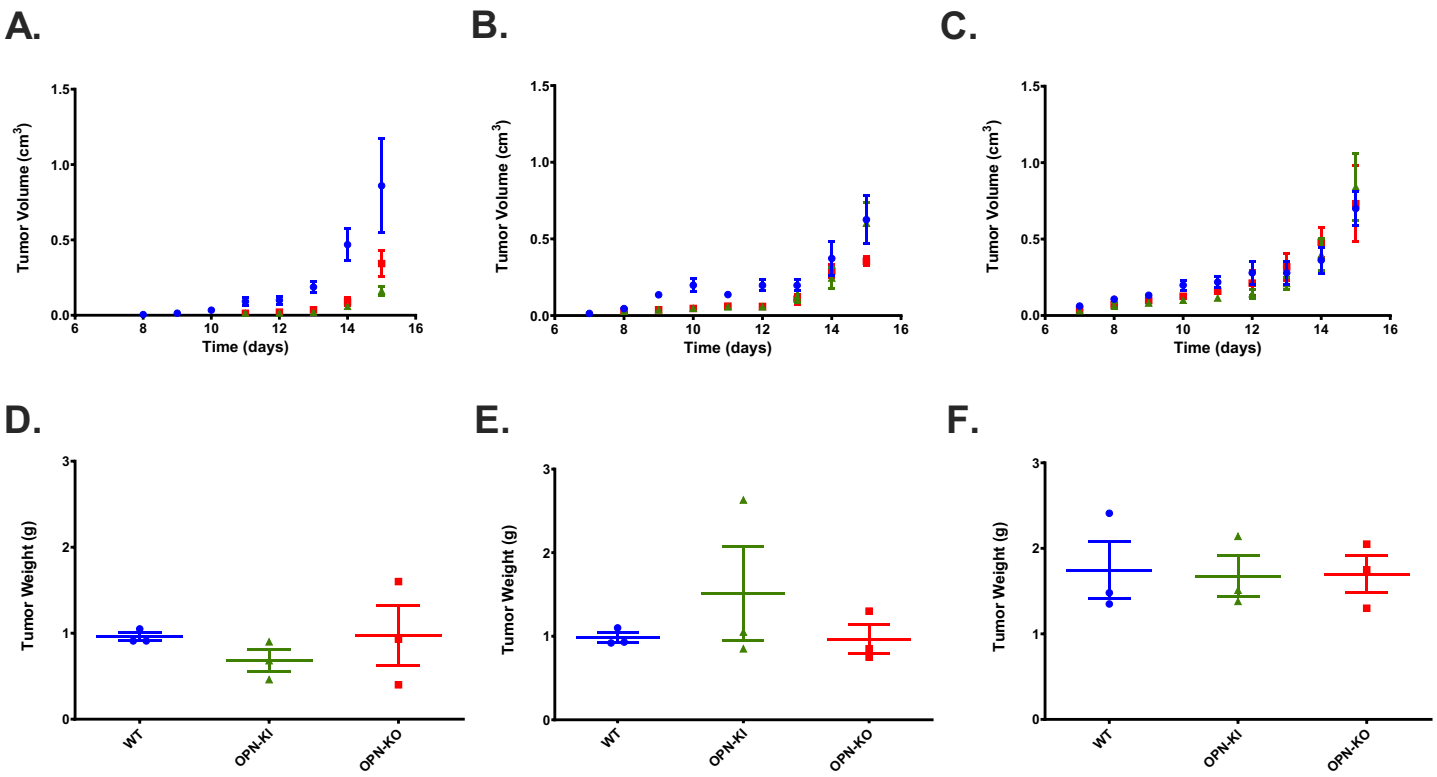

Supplementary Figure 8: No differences in B16 tumor growth between NOG-WT, NOG-OPN-KI and NOG-OPN-KI mice due to size of inoculum

Comparison of B16 tumor growth on NOG mice inoculated with different numbers of B16 cells. Growth rates of B16 tumors in (A-C; WT blue circles, NOG-OPN-KI green triangles and NOG-OPN-KO red squares), and weight of B16 tumors after sacrifice in NOG-WT (D), NOG-OPN-KI (E) and NOG-OPN-KO (F) following inoculation with $0.5x10^6$ (A & D), $1x10^6$ (B & E) and $2x10^6$ B16 cells (C & F) respectively. N=3 for each group. All data are shown as mean ± SEM. Data analyzed by ANOVA followed by Tukey post hoc test and showed no differences between groups.

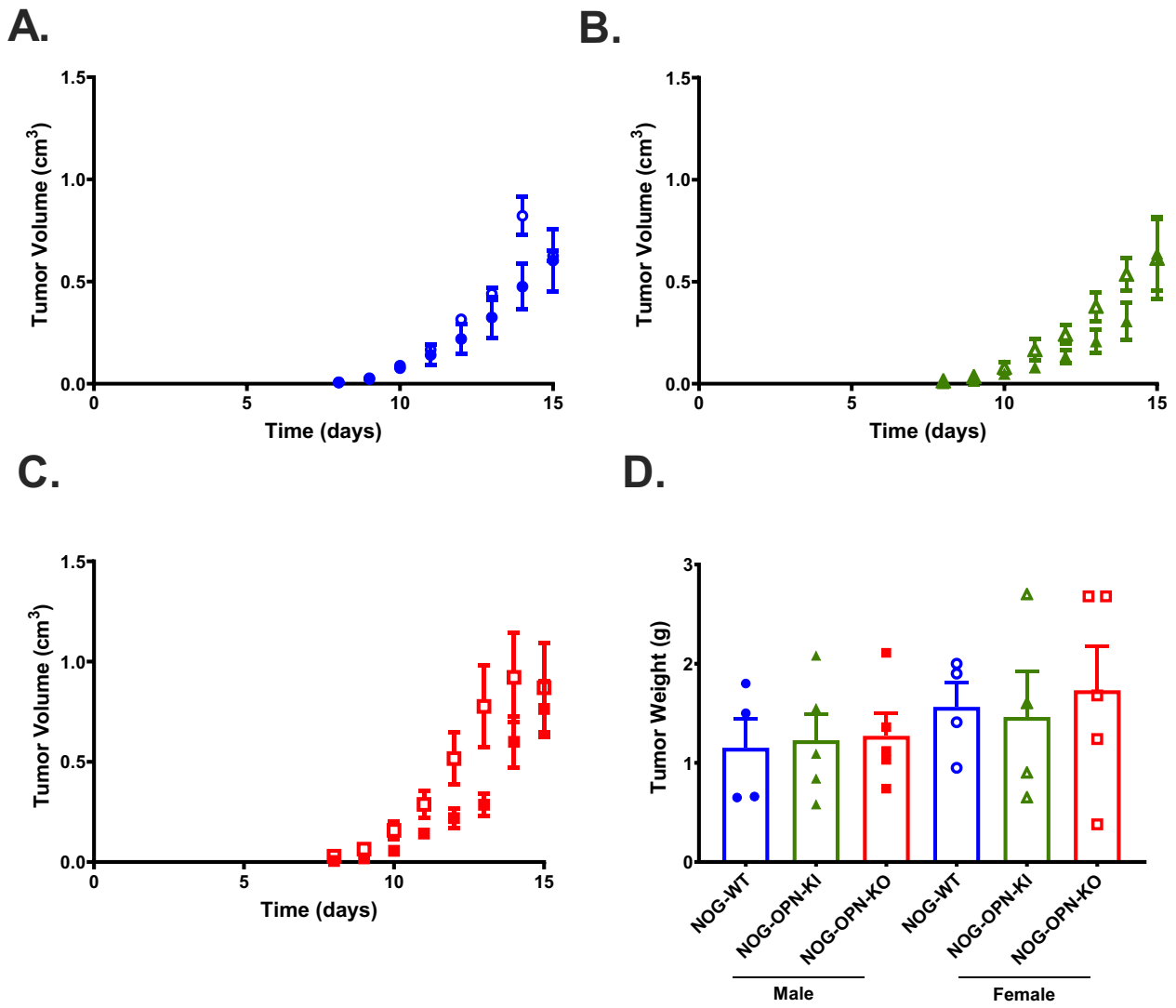

Supplementary Figure 9: No differences in B16 tumor growth between male and female NOG-WT, NOG-OPN-KI and NOG-OPN-KI mice

Comparison of B16 growth in male and female NOG mice. Growth rates of B16 tumors in male (closed symbols) or female (open symbols) NOG-WT (A), NOG-OPN-KI (B) and NOG-OPN-KO (C) mice, and weight of B16 tumors after sacrifice in male (closed symbols) or female (open symbols) NOG-WT, NOG-OPN-KI and NOG-OPN-KO mice (D). N=4 for NOG-WT and N=5 for NOG-OPN-KI and NOG-OPN-KO. All data are shown as mean ± SEM. Data analyzed by ANOVA followed by Tukey post hoc test and showed no differences between groups.

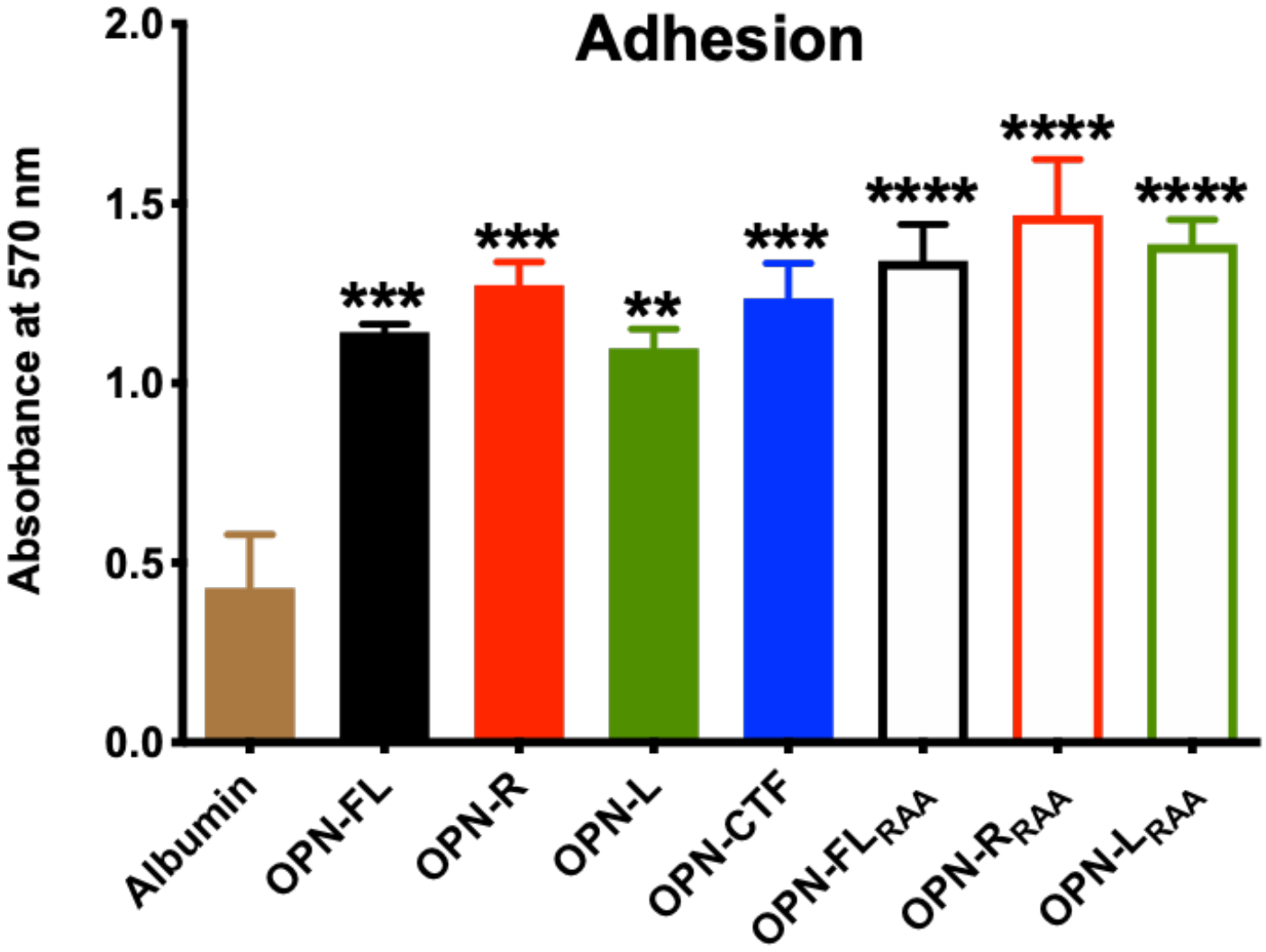

Supplementary Figure 10: Adherence of RAW cells is similar to different OPN fragments

Adhesion of RAW cells to different fragments of OPN. All data are shown as mean ± SEM. Data analyzed by ANOVA comparing to albumin followed by Dunnett's post hoc test. *: $p<0.05$, **: $p<0.01$, ***: $p<0.001$, ****: $p<0.001$. OPN-FL=OPN full length, OPN-R=OPN-Arg, OPN-L=OPN-Leu, OPN-CTF=OPN-C-terminal fragment. Subscript RAA denotes substitution of the RGD sequence by RAA in that OPN fragment.

Supplementary Table 1: Primers

StanfordU2 3R:	5’-TCTGAAACATAGTTCCCTAAGACATCAG-3’
NeoPCRF1:	5’-GGTTTCCAAATGTGTCAGTTTCATAGCC-3’
StanfordU2 5cko:	5’-ATCATCAATGCTTAGCCAAGCCAAG-3’

Supplementary Table 2: Antibodies

PE goat anti-mouse Integrin α9 Antibody	R & D systems	Cat. #: FAB3827P
PE rat anti-mouse Integrin β1 (CD29) Antibody	R & D systems	Cat. #: FAB2405P-100
PE anti-mouse CD49d (Integrin α4) Antibody	Affymatrix eBiosciences	Cat. #: 12-0492-82
PE goat IgG isotype control Antibody	R & D systems	Cat. #: IC108P
PE rat IgG2a Isotype Control Antibody	Tonbo biosciences	50-4321-U100
PE rat IgG2b isotype control Antibody	Tonbo biosciences	50-4031-U100
Brilliant Violet 421™ anti-mouse CD45 Antibody	BioLegend	Cat. #: 103133
PE anti-mouse CD206 (MMR) Antibody	BioLegend	Cat. #: 141706
Brilliant Violet 510™ anti-mouse I-A/I-E Antibody	BioLegend	Cat. #: 107635
PE/Cy7 anti-mouse CD11c Antibody	BioLegend	Cat. #: 117318
APC/Cy7 anti-mouse/human CD11b Antibody	BioLegend	Cat. #: 101226
Brilliant Violet 785™ anti-mouse F4/80 Antibody	BioLegend	Cat. #: 123141
PerCP/Cyanine5.5 anti-mouse CD38 Antibody	BioLegend	Cat. #: 102722
Brilliant Violet 650™ anti-mouse Ly-6G/Ly-6C (Gr-1) Antibody	BioLegend	Cat. #: 108441
EGR2 Monoclonal Antibody (erongr2), APC	Invitrogen	Cat. #: 17-6691-82
Sytox™ Green	BioLegend	Cat. #: 425303
Fc blocking antiCD16/32	Tonbo	Cat. #: 70-0161-U100
rat anti-mouse F4/80 monoclonal antibody	Biorad	Cat. #: MCA497RT
rabbit polyclonal anti–CD3 antibody	Abcam	Cat. #: 5690
Alexa Fluor 488 goat Anti-Rat IgG	Abcam	Cat. #: Ab150157